

Photocurrent Mechanisms of Low-Temperature Processed Polysilicon Thin-Film Transistors

¹ Yamina BOUREZIG, ¹ Khalid TOUMI, ¹ Badra BOUABDALLAH,
¹ Mohammed DEBAB, ² Baya ZEBENTOUT

¹ Laboratoire d'Elaboration et de Caractérisation de Matériaux,
Département d'Electronique. Université Djilali Liabès de Sidi Bel Abbès.22000, Algeria

² Laboratoire de Microélectronique Appliquée,
Département d'Electronique. Université Djilali Liabès de Sidi Bel Abbès.22000, Algeria

¹ Tel.: ++ 21391432862,

E-mail: a_bourezig@yahoo.fr

Received: 31 December 2012 /Accepted: 10 August 2013 /Published: 26 May 2014

Abstract: Steady state photocurrents have been measured in poly-Si TFTs fabricated from crystallized films deposited in an initially amorphous state by LPCVD technique. The transfer characteristics of poly-Si TFT change remarkably by illumination in the subthreshold and off-state regions. It is discovered that the photocurrent I_{ph} is more than three orders of magnitude greater than the dark currents. In the subthreshold and small negative V_{GS} regions, the photocurrent is attributed to thermionic emission of electrons over the GB barriers and ohmic conduction respectively. It depends on the gate bias and channel length. However, I_{ph} in high V_{GS} region is independent on these two parameters. It is therefore set only by the light-induced generation of electrons and holes. In addition, the photocurrent increases linearly with film thickness. The observed decrease for films thinner than 0.1 μm could be due to the increased influence of surface recombination at the poly-Si/SiO₂ interfaces. Copyright © 2014 IFSA Publishing, S. L.

Keywords: Polycrystalline-Silicon, TFT, LPCVD, Photocurrents, Photosensitivity, Grain boundaries.

1. Introduction

LOW-TEMPERATURE polycrystalline-silicon (LTPS) thin-film transistors (TFTs) have attracted much attention for active-matrix liquid crystal display and active-matrix organic light-emitting diode applications due to the high mobility and the capability of realizing integrated circuits on glass. It could reduce the difficulties of the connection of the surrounding circuits and the cost of the panel [1]. The photosensitivity of LTPS TFTs is a significant design consideration for achieving high-image-quality display panels. Thus, the photosensitive behavior of LTPS TFT current is of great interest.

Although poly-Si is generally recognized as being less photosensitive than *a*-Si: H, there does not

appear to be a consensus on the photosensitivity of poly-Si TFTs. There are reports of little or no photosensitivity [2, 3]. In this paper, we report on the gate bias effect on the photocurrent and show that the device photocurrents are appreciable and are controlled by the external bias voltages. The photocurrent mechanisms are systematically clarified. The dependence of photocurrent on channel length and active layer thickness is also characterized.

2. Experiments

All devices used in this study were n-channel auto-registered poly-Si TFTs fabricated on glass substrate. The Poly-Silicon formed by furnace

crystallization of amorphous Si deposited at 550 °C by LPCVD and crystallized at 625 °C was used for both the gate and channel layers. The gate oxide thickness was 150 nm of SiO₂ produced by APCVD. The source, drain and gate contact regions were doped n-type by phosphorus ion-implantation. Next, the hydrogenation was carried out in an inductively coupled RF plasma at 350 °C. The cross-sectional view of n-channel LTPS TFTs is shown in Fig 1. In this paper, the I(V) characteristics are measured under dark and illumination conditions. The illumination source for these measurements was a Schott KL1500 lamp with the light collimated and focused onto the devices with top-face white-light illumination.

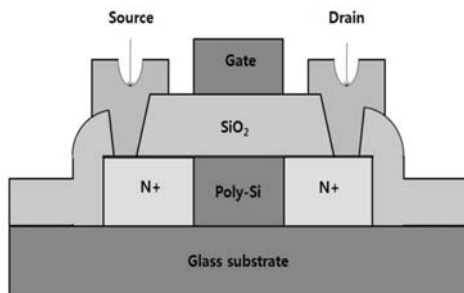


Fig. 1. Cross-sectional view of fabricated LTPS TFT.

3. Results and Discussion

Fig. 2a shows the drain current versus gate bias characteristics with $W/L = 50 \mu\text{m}/6 \mu\text{m}$ in the dark and with 10^5 lux top side white light illumination.

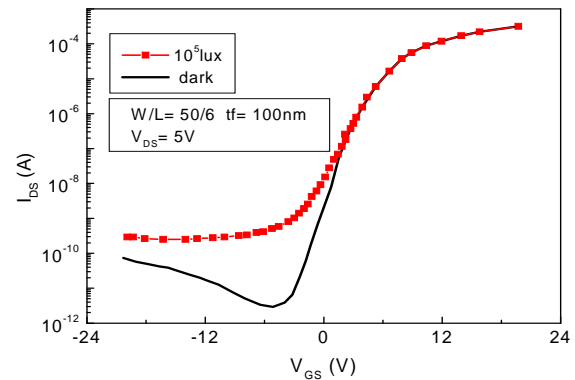
As can be seen, the photocurrent disappears under high positive gate voltages (over the threshold voltage), but only appears in the off state and subthreshold regions. Thus, large increase in drain current I_{DS} was observed in the subthreshold and off-state regions. These results can be understood by the contribution of photogenerated carriers to the total current.

The same figure indicates that the off current under illumination is less dependent on gate voltage in contrast to the dark current which is field enhanced [4]. This can be explained by the fact that, in off state region, the poly-Si TFT current is set only by the light induced generation of electrons and holes. Therefore, in this regime, there is no longer any influence of the gate voltage on the TFT drain current.

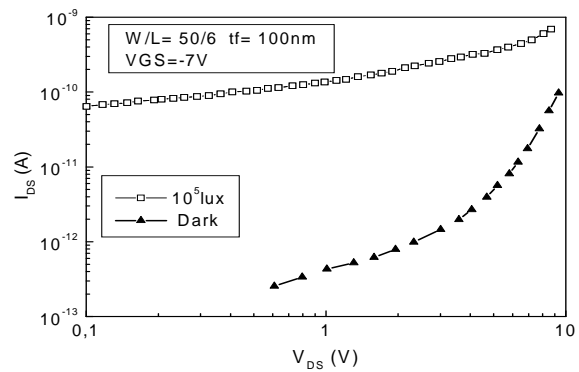
In Fig. 2b, the $(I_{DS})=f(V_{DS})$ characteristic under illumination shows a similarly weak bias dependence, while the dark current displays the expected exponential dependence on drain bias which is characteristic of the phonon assisted tunnelling mechanism [4].

To analyze the photocurrent of LTPS TFTs in detail, we further calculate I_{ph} from the curves. Thus, it can be taken that the total current I_{total} under

illumination is composed of two components: One is the current that is not caused by photo illumination (I_{Dark}), which is measured under dark state. In addition, the other part is illumination current (I_{ph}) which denotes the component induced by illumination. In this paper, we will consider the behavior of I_{ph} defined to be the difference between I_{total} and I_{Dark} only in the regions of interest.



(a)



(b)

Fig. 2. Characteristics of fully hydrogenated crystallized *a*-LPCVD poly-Si TFT measured in the dark and under white light illumination a: $I_{DS} = f(V_{GS})$, b: $I_{DS} = f(V_{DS})$ in the off-state.

3.1. Field Effects on I_{ph}

Fig. 3 shows the gate bias dependence of I_{ph} at $V_{DS} = 5$ V.

When put into the context of the dark current density, at several volts drain bias, of $2-6 \times 10^{-14}$ A/ μm obtained from this device and other low leakage TFTs [3, 4, 5], it is apparent that with ambient light intensities of 10^5 lux, the device photocurrent normalized with respect to channel width is equal to 1.8×10^{-10} A/ μm , leading to photo-to-dark current ratio higher than 10^3 .

As can be seen on Fig. 3, In the Off-state, the photocurrent is significantly higher than in the On-state, but still several decades lower than the peak value. It decreases when $|V_{GS}|$ increases. However, when $|V_{GS}|$ is large enough, I_{ph} becomes insensitive to the variation of the gate bias.

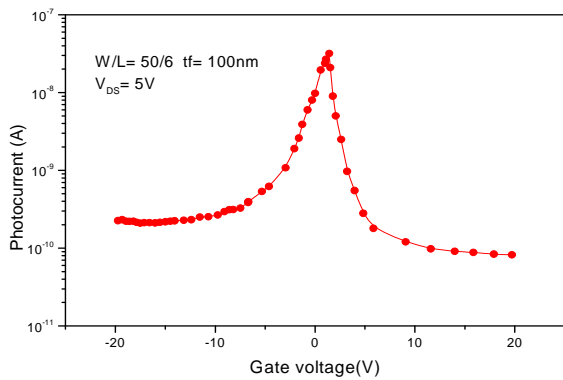


Fig. 3. Gate bias effect on photocurrent at $V_{DS} = 5$ V.

A previous report [6] confirms that the mechanisms of the photosensitivity for the LTPS TFT are closely related to the different defect distribution or density in the grain boundary, alike the case of the dark off current.

Based on this result, the photo-leakage current I_{ph} will be discussed. We consider that I_{ph} , as the dark current, is mainly dependent on deep level trap sites and is determined by the channel resistance R_{ch} and drain junction R_j . Depending on the gate and drain biases, the relative importance of R_{ch} and R_j can be different. At equilibrium, the channel resistance resulting from lower carrier concentration and mobility is very high and can sometimes be comparable with the junction resistance [7].

The deep traps at the grain boundaries have extremely low mobility and the potential barriers exist between the deep trap states and grain. The barrier appears to have various energies over which the photo-generated holes can be trapped. Illumination increases the number of electrons and holes. When $|V_{GS}|$ increases, more excess holes can be easily trapped at grain boundaries. Therefore, it is the trapping mechanism that causes the decrease of the photocurrent in the small negative V_{GS} region. Consequently, when the applied V_{GS} is not negatively large, the photocurrent can be assumed to be an ohmic current flowing through the polysilicon layer.

To support our assumption, the dependence of this current on drain voltage at low gate bias is shown in Fig. 4, which indicates that I_{ph} in this region varies linearly with V_{DS} . From the above description, it is obvious that I_{ph} is a resistive current.

With a further increase of V_{GS} , holes are induced to form a p-type channel region, and subsequently a reverse-biased p-n junction is formed between drain and channel. In that case, the photocurrent depends only on the light induced generation and recombination of electrons and holes in the drain pn junction depletion region. Note that for high negative voltages, the recombination rate can be neglected and the photocurrent is therefore set only by the light induced generation of electrons and holes. This can explain why, in this regime, there is no longer any influence of the gate voltage on the TFT photocurrent as shown in Fig. 3.

With a further increase of V_{GS} , holes are induced to form a p-type channel region, and subsequently a reverse-biased p-n junction is formed between drain and channel. In that case, the photocurrent depends only on the light induced generation and recombination of electrons and holes in the drain pn junction depletion region. Note that for high negative voltages, the recombination rate can be neglected and the photocurrent is therefore set only by the light induced generation of electrons and holes. This can explain why, in this regime, there is no longer any influence of the gate voltage on the TFT photocurrent as shown in Fig. 3.

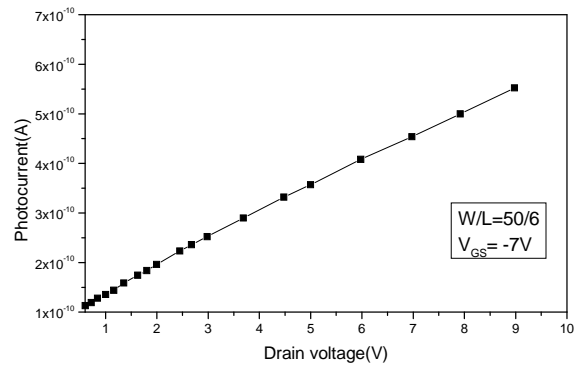


Fig. 4. Variation of photocurrent with drain bias voltage in the small negative V_{GS} region.

In the weak inversion regime (gate voltage lower than the threshold voltage), excess electrons can flow from source to drain because of the electron accumulation which enhances the injection over the potential barriers of the excess carriers. In this regime, the grain boundaries act as recombination centers. Some of the excess minority carriers cause the barrier height to be reduced by neutralizing the charge due to the majority carriers trapped at the grain boundary. This allows more current to flow. Thus, the photocurrent increases and reaches a maximum. We can clearly see a peak corresponding to the TFT weak-inversion regime, typically observed for small, positive gate voltage.

The TFT photocurrent disappears in the strong-inversion regime, as expected, because of the significant effect of the gate voltage on the concentration of accumulated carrier. In such case, the dark current dominates the photo-carrier collection.

3.2. Channel Length Effect

Fig. 5 indicates the channel length dependence of photocurrent under different gate biases.

In off state, when the gate bias V_{GS} is smaller than the flat band voltage, the photocurrent decreases as L increases. As mentioned above, the photocurrent is assumed to be an ohmic current flowing through the

polysilicon layer. Moreover, it has been reported [8], that the channel resistance, R_{ch} is mainly related to the crystallinity of the channel film. The better crystallinity of the channel film leads to the lower R_{ch} value.

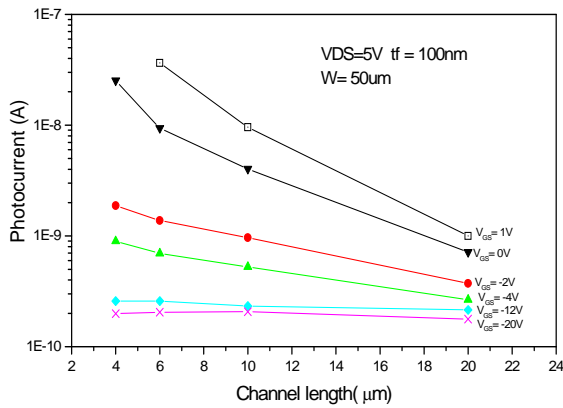


Fig. 5. Photocurrents as a function of channel length at different gate biases.

Generally, the crystallinity of the channel film is dominated by the grain boundary density in the channel film [9]. As a result of few grain-boundary numbers in the short channel length, the R_{ch} is reduced with decreasing channel length. Therefore, a short channel length is expected to result in higher photocurrent value.

However, when the applied V_{GS} is negatively large enough, the photocurrent is caused by the light-induced generation of electron-hole pairs in the depletion region near the drain. Consequently, the photocurrent is nearly independent on channel length. In the subthreshold region, the photocurrent I_{ph} is found to be channel length dependent. It decreases with an increase in channel length as a result of the large grain-boundary numbers in long channel which enhance the recombination of excess minority carrier (electrons) with trapped majority carriers (holes), making reduced the photocurrent.

3.3. Film Thickness Effect

The second factor affecting the photocurrent is the film thickness. The influence of the film thickness on the photocurrent depends on the TFT operation regime to be considered. A previous study [10] indicates that, in off state regime, the TFT photocurrent depends strongly on the film thickness when V_{GS} is relatively small. It increases with poly-Si thickness and decreases with poly-Si density-of-states. In contrast, in high V_{GS} region, the photocurrent depends only on the light-induced generation of electron-hole pairs in the depletion region near the drain. It increases with the illumination intensity and with the pn junction area.

Based on these results, we investigate the effect of film thickness only in the subthreshold region. In addition, in the absence of a qualitative difference between different gate voltages for this regime as shown in Fig. 5, the results are reported on Fig. 6 for zero gate voltage only.

With the film thicknesses used in this work, the total number of photons absorbed will increase approximately linearly with thickness giving a corresponding linear increase of photocurrent with film thickness.

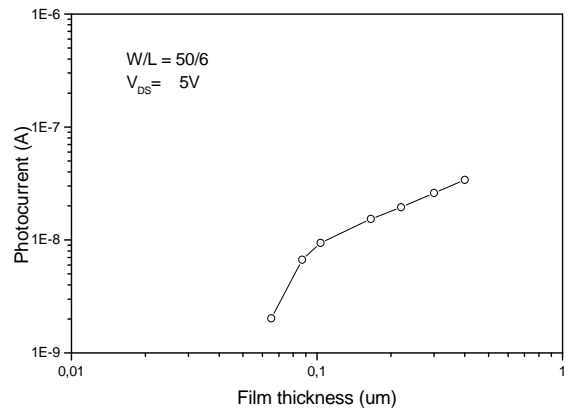


Fig. 6. Variation of Photocurrents with Poly-Si film thickness.

The obtained results can be explained by the variation of the traps density with film thickness. In addition, it is well known that the structural and electronic properties of the polycrystalline deposition films are improved during the layer growth [11]. In subthreshold regime, as previously mentioned, the grain boundaries act as recombination centers. Therefore, more recombination centers for electrons and holes in thin films can increase the carriers recombination rate. Due to this important factor, so the photocurrent decreases. This assertion can explain the behavior of the photocurrent for film thicknesses greater than $0.1 \mu\text{m}$, and confirms that the basic quantity affecting I_{ph} is the density of the defects in the polysilicon material.

A sharper than linear drop is seen in films less than $0.1 \mu\text{m}$ thick. This result is consistent with the experimental observations of negligible photocurrent in devices fabricated using 250 \AA thick poly-Si layers [12].

The observed strong decrease in photocurrent density suggests both a reduction of bulk recombination lifetime, due to the defects within the film and increased relative influence of interface recombination in the thinner films. Indeed, most of the photo-electrons are recombined at both poly-Si/ SiO_2 interface and grain boundaries before reaching the drain electrode. Consequently, only a small part of the photocarriers has contribution to I_{ph} . In such case, both the interface and bulk disorder affect the photocurrent in thin films.

4. Conclusion

Photocurrents have been measured in poly-Si TFTs. Both the gate and channel layers are formed by furnace crystallization of amorphous Si deposited at 550 °C by LPCVD and crystallized at 625 °C. The dependence of photocurrent on gate bias voltages, channel length, and active layer thickness is investigated. The results show that, under top face illumination with white light at an intensity of 10^5 lux, the photocurrent is more than three orders of magnitude greater than the dark current.

Under positive V_{GS} , some of the excess minority carriers recombine with the majority carriers trapped at the grain boundary. This reduces the potential barriers allowing more photo-electrons to flow. Therefore, the photocurrent attributed to thermionic emission process increases and reaches a maximum corresponding to the TFT weak-inversion regime.

In off state, and in contrast to the dark current, the photocurrent decreases with the increase of gate bias in small negative gate region. This behavior is attributed to trapping mechanism. The current in this region is assumed to be ohmic. In both positive and small negative bias, the photocurrent depends on channel length.

However, when V_{GS} is large enough, the photocurrent is attributable to pure thermal generation. This can explain why, in this regime, there is no longer any influence of the gate voltage or channel length on the TFT photocurrent.

In addition, the photocurrent increases with film thickness. For film thicknesses greater than 0.1 μm , this behavior can be related to the variation of the grain boundaries with film thickness. However, for films thinner than 0.1 μm , the strong decrease of photocurrent with decreasing film thickness is due to both the interface and bulk disorder.

References

- [1]. Y. H. Tai, C. C. Pai, B. T. Chen, and H. C. Cheng, A source-follower type analog buffer using poly-Si TFTs with large design windows, *Electronics Letters*, Vol. 26, Issue 11, 2005, pp. 813–881.
- [2]. K. Masumo, M. Kunigita, S. Takafuji, and M. Yuki, Low temperature fabrication of poly-Si TFT by laser

induced crystallization of a-Si, *Journal of Non-Crystalline Solids*, Vol. 115, Issue 1-3, 1989, pp. 147-149.

- [3]. H. Ohshima, and S. Morozumi, High performance poly-Si TFT for LCDs, in *Proceedings of the International Conference on Solid State Devices and Materials (ISSDM'91)*, Yokohama, 1991, pp. 577-579.
- [4]. J. R. Ayres, S. D. Brotherton, and N. D. Young, Low temperature poly-Si for LCD addressing, *Optoelectronics. Devices and Technologies*, Vol. 7, Issue 2, 1992, pp. 301-320.
- [5]. S. D. Brotherton, J. R. Ayres, and N. D. Young, Characterization of low temperature poly-Si thin film transistors, *Solid State Electronics*, Vol. 34, Issue 7, 1991, pp. 671-679.
- [6]. Y. Hsiang Tai, Y. F. Kuo, and Y. H. Lee Photosensitivity Analysis of Low-Temperature Poly-Si Thin-Film Transistor Based on the Unit-Lux-Current, *IEEE Transactions on Electron Devices*, Vol. 56, Issue 1, 2009, pp. 50-56.
- [7]. F. Qian, D. M. Kim, G. H. Kawamoto, Inversion/accumulation- Mode Polysilicon Thin Film Transistors Characterization and Unified Modeling, *IEEE Transactions on Electron Devices*, Vol. 35, Issue 9, 1988, pp. 1501-1509.
- [8]. C. L. Fan, T. H. Yang, Y. C. Chen and J. Lin, Effects of laser activation on device behaviour for poly-Si thin-film transistors with different channel lengths, *Electronics Letters*, Vol. 42, Issue 6, 2006, pp. 374-375.
- [9]. N. Yamauchi, J. Hajjar, and R. Reif, Polysilicon thin-film transistors with channel length and width comparable to or smaller than the grain size of the thin film, *IEEE Trans. Electron Devices*, Vol. 38, Issue 1, 1991, pp. 55–60.
- [10]. J. Kanicki, and S. Martin, Hydrogenated Amorphous Silicon Thin-Film Transistors, eds. C. R. Kagan and P. Andry (Marcel Dekker, Inc., New York), 2003.
- [11]. M. Amrani, Z. Benamara, M. Chellali, S. Tizi, T. M. Brahim, Experimental study and two-dimensional modeling of avalanche breakdown voltage in polycrystalline silicon p-n junctions, *Journal of Applied Physics*, Vol. 101, Issue 10, 2007, pp. 104509.
- [12]. S. Morozumi, R. Araki, H. Ohshima, M. Matsuo, T. Nakazawa, and T. Sato, Low temperature processed poly-Si TFT and its application to large area LCD, in *Proceedings of the 6th International Display Research Conference (IDRC'86)*, Tokyo, Japan, 1986, pp. 196-199.